Soft Matter

PAPER

View Article Online
View Journal | View Issue

Cite this: *Soft Matter*, 2026, 22, 3063

Electromechanical responses in water-rich self-assembled amphiphile gels and hydrated ionogels: reassessing piezoelectric attributions

Erica Pensini *[a] and Alejandro G. Marangoni [b]

Water-rich, self-assembled amphiphile gels have recently been reported to exhibit electrical responses under mechanical deformation and hysteretic cyclic voltammetry behavior, leading to their interpretation as piezoelectric or ferroelectric soft materials. Such claims are particularly compelling given the relevance of hydrated, compliant electromechanical materials to biological, biomedical, and soft-sensing applications. However, in ion-containing soft matter, the electrical signatures commonly used to infer piezoelectricity are not uniquely diagnostic and may arise from multiple coupled mechanisms. Here, we re-examine the electromechanical behavior of fatty acid–amine, fatty acid–amino acid, and surfactant–fatty alcohol hydrogels previously described as piezoelectric. We show that capacitive cyclic voltammetry responses and mechanically induced voltage or current transients can be rationalized within a broader framework of electromechanical coupling in hydrated ionic gels, encompassing electrokinetic charge redistribution, electrode double-layer and interfacial effects, and strain-dependent dielectric responses, in addition to intrinsic polarization. As an instructive non-amphiphile comparator, ionotropically crosslinked carboxymethyl cellulose gels exhibit closely analogous electrical signatures only in the presence of multivalent ionic crosslinkers, reinforcing the non-uniqueness of piezoelectric interpretations in hydrated ionic systems. To clarify these distinctions, we introduce a minimal coupled electromechanical model that explicitly separates instantaneous elastic polarization from rate-dependent ionic contributions and identifies their distinct experimental signatures. We further propose discriminating experiments required to unambiguously distinguish intrinsic piezoelectricity from electrokinetic and interfacial effects. This reassessment does not diminish the functional relevance of these materials; rather, it provides a rigorous mechanistic foundation for their continued development as soft electromechanical transducers for sensing, biointerfacing, and biomedical applications.

Received 18th January 2026,
Accepted 30th March 2026

DOI: 10.1039/d6sm00047a

rsc.li/soft-matter-journal

1. Introduction

Electromechanical coupling in soft, hydrated materials has attracted growing interest due to its relevance in biological tissues, soft sensors, and biointerfacing technologies.[1–4] Unlike classical piezoelectric solids, which are typically rigid, crystalline, and weakly conductive, many biological and biomimetic systems are water-rich, compliant, and ionically conductive.[5,6] Understanding how mechanical deformation gives rise to electrical signals in such materials is therefore of fundamental importance, both for interpreting experimental observations and for guiding the design of functional soft matter.

In recent years, several classes of self-assembled amphiphile gels and polymeric hydrogels have been reported to exhibit electrical responses under mechanical deformation and hysteretic features in cyclic voltammetry (CV) measurements.[7–12] These systems include fatty acid–amine and fatty acid–amino acid hydrogels, surfactant–fatty alcohol–water gels, and crosslinked polymer hydrogels.[7–10,12] They are typically characterized by high water content, ionic character, and mesoscopic order (*e.g.*, lamellar or ribbon-like assemblies). Mechanically induced voltage or current signals, together with capacitive or hysteretic current–voltage responses, have motivated interpretations in terms of piezoelectricity and, in some cases, ferroelectric-like behavior—an especially compelling conclusion given the scarcity of water-rich materials exhibiting intrinsic polarization-based electromechanical transduction.

However, in ion-containing soft matter, the electrical signatures commonly used to infer piezoelectricity are not uniquely diagnostic.[13] Bone provides a useful example: while collagen is intrinsically piezoelectric, electrical signals measured during mechanical loading of hydrated bone can also arise from

[a] *Department of Civil Engineering, University of Guelph, Guelph, Ontario, Canada. E-mail: epensini@uoguelph.ca*
[b] *Department of Food Science, University of Guelph, Guelph, Ontario, Canada*

electrokinetic mechanisms such as streaming potentials associated with fluid flow.[14] Macroscopic "piezoelectric" measurements on wet bone should therefore be interpreted as potentially composite mechanoelectric responses. In hydrated gels, CV can be strongly influenced by electrical double-layer charging at electrode interfaces, electrode polarization, and ionic migration within the material.[15] Likewise, electrical signals generated during mechanical deformation may arise not only from intrinsic polarization but also from strain- or pressure-driven ion redistribution, as well as changes in electrode–gel contact conditions during loading.[16,17] These coupled processes can produce reproducible electrical responses that closely resemble piezoelectric-like signatures, particularly in compliant, highly hydrated systems. Critically, such contributions can also account for systematic dependencies on loading rate, ionic strength, and electrode material that are difficult to reconcile with a purely intrinsic piezoelectric origin.

Accordingly, cyclic voltammetry and stress-generated electrical measurements, while useful screening tools, cannot—when considered in isolation—be taken as definitive proof of intrinsic piezoelectric polarization in hydrated ionic soft matter.

In our previous studies, "piezoelectricity" was used as an operational descriptor for the electromechanical behavior of self-assembled amphiphile gels and crosslinked polymer hydrogels based on these experimentally accessible signatures.[7,9,10,12] While this terminology was consistent with prevailing interpretations in related areas, it is timely to examine whether the available evidence uniquely supports an intrinsic piezoelectric origin, or whether a broader framework of electromechanical coupling provides a more consistent physical description.

The objective of the present work is therefore not to discount the functional relevance of electromechanical responses in these materials, but to clarify their mechanistic origin. We re-examine fatty acid–amine, fatty acid–amino acid, and surfactant–fatty alcohol hydrogels within a unified framework that explicitly accounts for ionic transport, interfacial effects, and viscoelasticity alongside possible intrinsic polarization. By highlighting the non-uniqueness of commonly used piezoelectric indicators in hydrated ionic gels, we aim to establish a more rigorous basis for interpreting experimental observations.

To this end, we first summarize the electromechanical signatures reported across these amphiphile gel systems, focusing on their shared phenomenology. We then discuss why CV and mechanically induced electrical signals are insufficient, on their own, to establish intrinsic piezoelectricity in water-rich soft matter. Building on this analysis, we introduce a minimal coupled electromechanical model that separates instantaneous elastic polarization from rate-dependent ionic contributions and predicts distinct experimental signatures for each mechanism. Finally, we outline discriminating experimental strategies required to resolve these contributions in future studies.

By reframing the discussion in terms of electromechanical coupling rather than categorical material classification, this work provides a foundation for the rational development of soft, hydrated electromechanical materials. Regardless of the dominant microscopic mechanism, the ability of these systems to transduce mechanical deformation into electrical signals remains of significant interest for sensing, biointerfacing, and biomedical applications.

2. Summary of reported electromechanical signatures in self-assembled amphiphile gels

A series of recent studies reported electromechanical responses in water-rich, self-assembled amphiphile gels formed from chemically distinct but structurally related systems, including fatty acid–amine hydrogels, fatty acid–amino acid hydrogels, surfactant–fatty alcohol–water gels and cross-linked polymer gels. Despite differences in molecular composition, these materials share several defining characteristics: high water content, ionic functionality, self-assembled mesophase organization, and mechanical compliance. This section summarizes the key experimental observations reported across these systems, focusing on their common phenomenology.

2.1 Fatty acid–amine and fatty acid–amino acid hydrogels

Hydrogels formed by combining oleic acid with small amines (*e.g.*, ethanolamine) or amino acids (*e.g.*, lysine, arginine) and up to $\approx$90 wt% water were shown to self-assemble into lyotropic liquid-crystalline mesophases. Lamellar organization was reported for systems containing oleic acid with monoethanolamine, diethanolamine, or aminomethylpropanol at high water content.[7,8] Depending on composition and water fraction, lamellar or columnar hexagonal phases were also observed in systems containing methyldiethanolamine or aminoethoxyethanol,[8] as well as in lysine-based formulations.[9] Structural characterization using polarized light microscopy and X-ray scattering indicated anisotropic organization across microscopic and mesoscopic length scales, with ribbon-like or bundled lamellar morphologies reported for some compositions.[7–9] These gels typically exhibited pronounced viscoelastic behavior.

Electrically, these systems displayed reproducible hysteretic current–voltage loops in cyclic voltammetry, often described as predominantly capacitive. Nonzero current near zero applied potential and scan-rate-dependent loop shapes were observed, with additional sensitivity to electrode configuration. These features were interpreted as indicative of polarization-related charging processes.

Under uniaxial compression between electrodes, transient electrical signals—reported as voltage in open-circuit configurations or current in short-circuit configurations—were detected. Signals typically appeared upon application or release of load and decayed over time after unloading (*i.e.*, once the applied force was removed), with relaxation typically occurring over seconds to minutes. The generation of electrical transients in the absence of an externally applied field motivated interpretation in terms of piezoelectric responses.

2.2 Surfactant–fatty alcohol–water hydrogels

Subsequent work extended these observations to surfactant-based systems, including zwitterionic and anionic surfactants

combined with long-chain fatty alcohols in water. These formulations also formed structured, water-rich gels exhibiting lamellar or C_P cubic mesophase ordering and mechanical softness comparable to the fatty acid–based systems.[12]

Similar to the fatty acid–amine and fatty acid–amino acid gels, surfactant–fatty alcohol hydrogels exhibited hysteretic cyclic voltammetry responses consistent with capacitive behavior. Electrical signals were again generated upon mechanical compression and release, with magnitudes and temporal profiles that depended on temperature and loading conditions; decay after unloading typically occurred over seconds to minutes. The observation of analogous behavior in chemically distinct amphiphile systems suggested that the underlying phenomenon is not specific to a particular molecular pairing, but instead associated with broader features such as ionic character, hydration, and self-assembled structure.

2.3 Polyelectrolyte polysaccharide gels: CMC crosslinked with Cu^{2+} as an instructive comparator

To underscore that the electrical signatures discussed above are not specific to self-assembled amphiphile mesophases, closely analogous behavior is also observed in ionotropically crosslinked polyelectrolyte hydrogels. Carboxymethyl cellulose (CMC), a carboxylate-bearing polysaccharide, forms coordination-crosslinked networks in the presence of multivalent cations such as Cu^{2+}, with Cu^{2+} binding to carboxylate sites and thereby altering both network mechanics and ionic transport pathways.[18]

In our measurements, CMC hydrogels prepared with $CuCl_2$ exhibit (i) stable, repeatable current generation under cyclic pressure loading and (ii) reproducible hysteretic current–voltage responses under cyclic voltammetry, including nonzero current near zero applied potential. These features are not observed in the absence of $CuCl_2$, indicating that multivalent-ion coordination and the resulting ionic environment are essential to the observed electromechanical response.[10] In addition, the response depends on the ionic crosslinking environment rather than arising generically from the polymer itself: published measurements showed that CMC gels crosslinked with $CuSO_4$ were markedly less capacitive and less mechanically responsive than those crosslinked with $CuCl_2$.[10] Such behavior does not by itself uniquely assign a microscopic mechanism, since changing the crosslinking salt can also alter gel structure, cohesion, and mechanics. However, it reinforces the central point of the present work: in hydrated ionic soft matter, electrically active responses commonly attributed to intrinsic piezoelectricity can be strongly conditioned by ionic composition and associated interfacial or transport phenomena.

Mechanistically, this behavior is consistent with interpretations based on piezoionic (piezoionic-like) coupling in hydrated ionic media, in which pressure gradients and strain-driven fluid/ion redistribution generate transient ionic currents and voltages without requiring intrinsic ferroelectric switching.[16] Beyond bulk transport, gel–electrode interfaces can contribute substantially through electrical double-layer charging and contact-dependent interfacial impedance, which can produce scan-rate-dependent hysteresis and baseline offsets in electrochemical measurements of soft, ionically conductive gels.[19]

The CMC–Cu^{2+} system therefore provides an instructive comparator: a highly hydrated, ionically conductive gel with fixed charges and mobile ions that reproduces the two canonical signatures often taken as evidence of piezoelectricity, while also showing clear sensitivity to ionic crosslinking conditions. This reinforces that these signatures are not uniquely diagnostic in hydrated ionic soft matter.

2.4 Common phenomenological features across systems

Across the reported amphiphile systems—and in ionotropically crosslinked polyelectrolyte comparators such as CMC–Cu^{2+}—a consistent phenomenology emerges despite substantial differences in molecular composition and mesoscale structure. First, the materials are highly hydrated and ionically conductive, with charged or zwitterionic functional groups and mobile ions present throughout the gel matrix. Second, amphiphile formulations often exhibit mesoscopic structural anisotropy (*e.g.*, lamellar or hexagonal self-assembly and, in some cases, higher-order ribbon-like organization), whereas CMC-based networks are coordination-crosslinked yet remain mechanically compliant and water-rich. Third, in both classes the mechanical response is soft and viscoelastic, with significant time-dependent relaxation under applied stress.

From an electrical standpoint, two signature families recur across systems: (i) hysteretic, scan-rate-dependent current–voltage loops in cyclic voltammetry, frequently including nonzero current near zero applied potential; and (ii) reproducible voltage or current transients generated during mechanical loading and unloading, often with time-dependent decay under held deformation. These signatures are reproducible across multiple formulations, establishing electromechanical responsiveness as a genuine and general property of hydrated ionic gels. At the same time, their recurrence in chemically and structurally distinct systems suggests that they may arise from general features of hydrated ionic soft matter—mobile ion redistribution, electrode double-layer charging, contact-impedance modulation, and viscoelastic/poroelastic relaxation—either alone or superimposed on possible intrinsic polarization,[16,20–22] rather than uniquely diagnosing bulk piezoelectric or ferroelectric order. Consistent with this view, streaming-potential measurements in polysaccharide hydrogel films (*e.g.*, hyaluronic acid) demonstrate that pressure-driven ion transport in charged, water-rich gels can generate measurable voltages with systematic dependence on pH and ionic strength, providing a direct non-piezoelectric pathway for mechanoelectric signals.[17]

This convergence motivates the mechanistic analysis in the following section, where we examine why these signatures are non-unique and identify the additional evidence required to discriminate intrinsic polarization from electrokinetic and interfacial contributions.

3. Non-uniqueness of piezoelectric signatures in hydrated ionic soft matter

Before discussing the non-uniqueness of common electromechanical signatures in hydrated ionic soft matter, it is useful to define what an intrinsic piezoelectric mechanism would imply in these materials. In mechanistic terms, piezoelectricity corresponds to direct coupling between mechanical stress or strain and electric polarization in a material whose molecular, supramolecular, or mesoscopic organization lacks inversion symmetry. At the phenomenological level, this means that polarization contains a component directly coupled to stress or strain, in contrast to voltage generation arising indirectly from ion migration or interfacial charge reorganization. Thus, a hydrated amphiphile gel could exhibit an intrinsic piezoelectric response only if it possesses a net polar bias, for example through preferential alignment of dipolar or charged assemblies or anisotropic packing of fibrillar or lamellar domains. Under deformation, this broken-symmetry organization would undergo a reversible change in dipole density, dipole orientation, or charge separation, generating a change in polarization and therefore a measurable electrical signal.

In that intrinsic picture, the electrical output is a direct consequence of deformation-induced polarization rather than of mass transport. The response should therefore track the applied mechanical perturbation on the timescale of elastic deformation, reverse with the sign of stress or strain, and, under maintained load, remain tied to the sustained stressed state rather than decaying primarily through ionic redistribution. By contrast, hydrated ionic gels also contain mobile ions, percolated aqueous pathways, electrical double layers, and deformable gel–electrode contacts. Mechanical loading can therefore drive ion redistribution, streaming potentials, deformation potentials, space-charge accumulation, interfacial charging, and contact-capacitance changes, each of which can generate voltage or current outputs without requiring intrinsic piezoelectric polarization.

The central interpretive challenge is therefore not whether a piezoelectric contribution is conceivable, but whether the measured signal can be uniquely assigned to stress-coupled polarization of a non-centrosymmetric organization rather than to relaxational electrokinetic and interfacial processes. This distinction is especially important here because similar electrical signatures recur across the amphiphile gels and the CMC–Cu^{2+} comparator and frequently depend on ionic conditions and electrode interfaces. In the discussion that follows, we examine why these readouts are not unique in water-rich ionic materials and identify the mechanistic evidence required to distinguish intrinsic polarization from electrokinetic and interfacial contributions.

3.1 Cyclic voltammetry and capacitive hysteresis in ionic gels

In classical piezoelectric and ferroelectric solids, hysteresis observed in electrical measurements is often attributed to polarization charging, switching, or relaxation. Cyclic voltammetry has therefore been widely used as an initial diagnostic of polarization-related phenomena in electroactive materials. However, in hydrated ionic gels, CV responses are strongly influenced by additional processes that can produce qualitatively similar hysteretic behavior.

One dominant contribution arises from the formation of electrical double layers (EDL) at the gel–electrode interface.[22] In the presence of mobile ions, an applied potential drives ion accumulation near the electrodes, generating non-faradaic capacitive currents that scale with scan rate and electrode area[23–25] and depend on electrolyte properties *via* EDL structure and transport.[23,26] These currents can persist even in the absence of bulk polarization and may produce apparent offset currents near zero applied potential. This is exemplified by the CMC–$CuCl_2$ CV trace (tilted, rounded hysteresis with appreciable current near the origin),[10] which is consistent with electrode double-layer charging and transport-limited ionic polarization superimposed on finite bulk/interfacial conductance, and corresponds to the electrokinetic/interfacial archetype summarized in Fig. 1b and c.

In redox-active ionic environments, additional pseudocapacitive/faradaic contributions may coexist with double-layer charging; for example, multivalent-ion crosslinkers can introduce redox chemistry or mixed-potential behavior that further accentuates hysteresis and apparent "offset" currents.[27]

Electrode polarization and contact impedance further complicate interpretation. Soft, deformable gels can exhibit variable wetting, contact area, and local pressure at the electrode interface, all of which influence interfacial capacitance and resistance.[28–33] More generally, imperfect interfacial contact—*e.g.*, interfacial voids or air gaps—can dominate the interfacial (charge-transfer) impedance, a point emphasized in solid–solid electrochemical interfaces and directly relevant to soft contacts where partial wetting creates voids.[34,35] Consequently, small changes in wetting and contact conformity can strongly modulate measured electrochemical signals even when bulk properties are unchanged. As a result, CV loop shape and magnitude may depend sensitively on electrode material, surface preparation, and geometry, without reflecting changes in the intrinsic bulk properties of the gel.

In addition, Maxwell–Wagner–Sillars (MWS) relaxation is an interfacial (space-charge) polarization mechanism in heterogeneous media, where contrasts in conductivity and/or permittivity drive charge accumulation at internal interfaces (often described as barrier-layer polarization), producing a slow, dispersive capacitive response that becomes prominent at low frequencies (or under slow electrical protocols).[36–38] Ionic migration within the gel can therefore give rise to space-charge polarization (including MWS-type interfacial polarization), particularly under low scan rates, introducing hysteresis associated with delayed ionic redistribution rather than polarization switching.[36,37,39] Accordingly, hysteretic CV signatures in hydrated ionic gels are non-unique and must be interpreted with caution; Fig. 1 summarizes how intrinsic polarization and electrokinetic/interfacial mechanisms can yield qualitatively similar loops. These effects predict scan-rate, ionic-strength, and electrode-dependences that can mimic

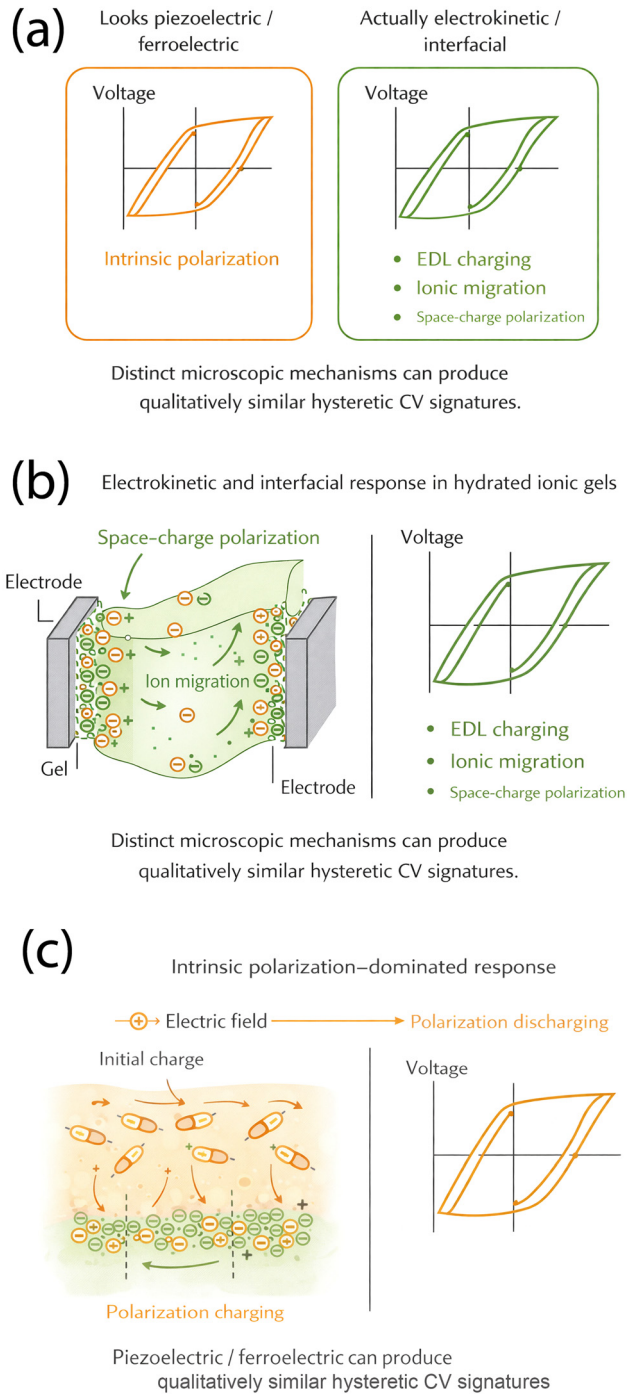

Fig. 1 Schematic illustration of distinct microscopic mechanisms that can produce qualitatively similar hysteretic cyclic voltammetry (CV) responses in hydrated, ionically conductive soft matter. (a) Comparison of phenomenological signatures, highlighting that distinct microscopic mechanisms—intrinsic polarization *versus* ionic and interfacial effects—can give rise to similar hysteretic CV loops. (b) Electrokinetic and interfacial response in hydrated ionic gels, where CV hysteresis originates from electrical double-layer charging at the gel–electrode interface, finite ionic mobility, and space-charge polarization during voltage sweeps. (c) Intrinsic polarization–dominated response, in which the measured current arises primarily from polarization charging and discharging under an applied electric field, as typically assumed for ideal piezoelectric or ferroelectric materials. This non-uniqueness underscores the need for complementary electromechanical measurements and mechanism-discriminating experiments when interpreting CV signatures in water-rich, ionically conductive materials. The CMC–$CuCl_2$ comparator exhibits a tilted, rounded hysteretic CV loop consistent with the electrokinetic/interfacial archetype shown in (b) (and the comparison summarized in (a)).

polarization-associated hysteresis even in the absence of intrinsic switching.

3.2 Mechanically induced electrical signals: piezoelectric *versus* electrokinetic origins

Mechanically induced electrical signals in hydrated ionic materials are often interpreted as evidence of piezoelectricity, but such an assignment is only justified if the response can be linked specifically to stress-coupled polarization of a non-centrosymmetric structure.

In hydrated soft matter, mechanically induced voltage or current transients may arise from several non-piezoelectric mechanisms. Consistent with the interfacial and transport contributions discussed in Section 3.1, mechanically induced signals in hydrated ionic gels can reflect coupled ionic redistribution and electrode-interface effects, and are therefore not uniquely diagnostic of intrinsic piezoelectric polarization.[40,41] Mechanical compression or deformation of an ion-containing gel can drive redistribution of mobile ions relative to the polymer or amphiphile network,[16,17,20,40] leading to transient charge separation and the development of deformation or streaming potentials. These electrokinetic effects are well known in porous and soft materials and depend on factors such as ion mobility, pore structure, and solvent viscosity.[42,43] Importantly, the resulting electrical signals are typically time-dependent, relaxing as ionic equilibrium is re-established under constant deformation (and, in poroelastic gels, as pressure gradients dissipate through solvent flow).[21,44]

Changes in electrode–gel contact during mechanical loading provide an additional source of electrical transients. Compression can modify the effective contact area, local pressure, and interfacial capacitance at the electrode surface, producing reproducible signals even in the absence of bulk polarization changes.[28–31,33–35,40] This sensitivity to contact conditions parallels the dependence of CV loop shape on interfacial impedance noted in Section 3.1, and can mimic piezoelectric-like responses if not carefully controlled.

The viscoelastic nature of hydrated gels further contributes to time-dependent electromechanical behavior. Under applied stress, strain relaxation and solvent redistribution occur over characteristic timescales that can couple to ionic transport and dielectric response.[21,44] As a result, mechanically induced electrical signals may depend strongly on deformation rate, temperature, and hydration level—dependencies that differ from those expected for purely elastic, intrinsic piezoelectric polarization.

Taken together, these considerations imply that mechanically induced transients in hydrated ionic gels should be interpreted as composite electromechanical responses in which instantaneous polarization, ionic redistribution, and interfacial/contact dynamics may coexist—motivating the explicit

separation of elastic and relaxational contributions in the coupled framework introduced in Section 4.

3.3 Role of structural anisotropy and mesoscale organization

The mechanisms outlined in Sections 3.1 and 3.2—electric double layer/electrode polarization and transport-limited ionic redistribution under electrical bias or mechanical loading—are expected to be particularly pronounced in gels with mesoscale order and anisotropic microstructure. Self-assembled amphiphile gels often exhibit pronounced structural anisotropy, arising from lamellar ordering and, in some cases, higher-order ribbon-like or bundled morphologies. This was for instance observed in systems containing oleic acid and alkanolamines[7,8] or oleic acid and lysine,[9] as well as other hydrogels used as actuators and robots.[6] Such organization can enhance electromechanical responses by introducing directional mechanical stiffness, strain gradients, and potentially anisotropic transport pathways.[45] More generally, mesoscale heterogeneity is expected to concentrate deformation into mechanically 'weaker' or geometrically thinner regions, so that local strain can substantially exceed the applied macroscopic strain; in stretchable sensor design this 'heterogeneous strain distribution' is a recognized route to amplified electrical readout, with local strain governed by spatial variations in modulus and cross-section.[46] This same strain-localization logic provides a structure-based rationale for why lamellar/ribbon anisotropy in amphiphile gels can magnify electrokinetic and interfacial contributions discussed in Sections 3.1 and 3.2, even in the absence of intrinsic polarization switching.[46]

Structural anisotropy can amplify both intrinsic and extrinsic mechanisms. In the case of intrinsic polarization, anisotropic molecular packing may facilitate dipole alignment or collective polarization under stress. At the same time, anisotropy can enhance electrokinetic effects by directing ion migration or concentrating strain-induced pressure gradients along preferred pathways.[40,42,43] Mesoscale heterogeneity can also impose spatially nonuniform electrode contact pressures and local current pathways,[47,48] thereby modulating the interfacial impedance effects emphasized in Sections 3.1 and 3.2.

As a result, ordered lamellar or ribbon-like structures do not uniquely imply intrinsic piezoelectricity; rather, they can amplify multiple concurrent pathways by tuning the effective coupling and relaxation parameters (*e.g.*, α, τ, and C_{eff}, and potentially d) that govern the composite response.

3.4 Implications for interpretation

Taken together, these considerations demonstrate that the electrical signatures reported for water-rich amphiphile gels—namely capacitive cyclic voltammetry responses and mechanically induced electrical transients—are informative but not sufficient indicators of intrinsic piezoelectricity. In hydrated ionic soft matter, such signatures may arise from a superposition of intrinsic polarization, electrokinetic charge redistribution, interfacial capacitance, electrode polarization, and viscoelastic/poroelastic relaxation. Accordingly, cyclic voltammetry and stress/pressure-induced electrical measurements, while useful screening tools, cannot—when considered in isolation—be taken as definitive evidence of bulk piezoelectric or ferroelectric order.

This non-uniqueness motivates the need for a framework that explicitly distinguishes between instantaneous, elastic polarization and rate-dependent ionic and interfacial contributions. In the following section, we introduce a minimal coupled electromechanical model that captures these distinct pathways and provides a basis for interpreting existing observations and for designing experiments capable of resolving their relative contributions.

The physical mechanisms that can give rise to electrically active responses under mechanical deformation in hydrated amphiphile gels are summarized schematically in Fig. 2. As illustrated, intrinsic piezoelectric polarization, electrokinetic charge redistribution, and electrode-related interfacial effects can each produce electrical signals during mechanical loading, despite arising from fundamentally different microscopic processes. This conceptual separation motivates an explicit constitutive framework capable of distinguishing these contributions, which is developed in the following section.

4. A minimal coupled electromechanical framework

To rationalize the electromechanical behavior observed in water-rich amphiphile gels and to distinguish intrinsic polarization from ionic and interfacial effects, we introduce a minimal coupled framework that captures the essential physics without invoking unnecessary complexity. The framework is phenomenological in nature and draws on established constitutive descriptions of piezoelectric polarization, dielectric relaxation, and electrokinetic charge transport. Its purpose is not to derive electromechanical coupling from first principles or to provide a full multiphysics description, but rather to establish a physically transparent, lowest-order model capable of distinguishing intrinsic polarization from relaxational ionic contributions in hydrated soft matter.

4.1 Mechanical response of hydrated amphiphile gels

We consider a one-dimensional compression geometry, consistent with the experimental configurations used to probe electromechanical responses. For small deformations, the mechanical behavior of the gel is represented as linear viscoelastic (Kelvin–Voigt):

$$\sigma(t) = E\varepsilon(t) + \eta\dot{\varepsilon}(t) \quad (1)$$

where t is time, σ is the applied stress, ε is the strain, $\dot{\varepsilon}$ is the strain rate, E is an effective elastic modulus, and η is a viscous (damping) coefficient. This description captures both instantaneous elastic deformation and rate-dependent dissipation characteristic of hydrated gels.

4.2 Intrinsic polarization contribution

If intrinsic piezoelectric polarization is present, the leading-order electromechanical coupling is linear in stress:

$$P_{\mathrm{p}}(t) = d\sigma(t) \quad (2)$$

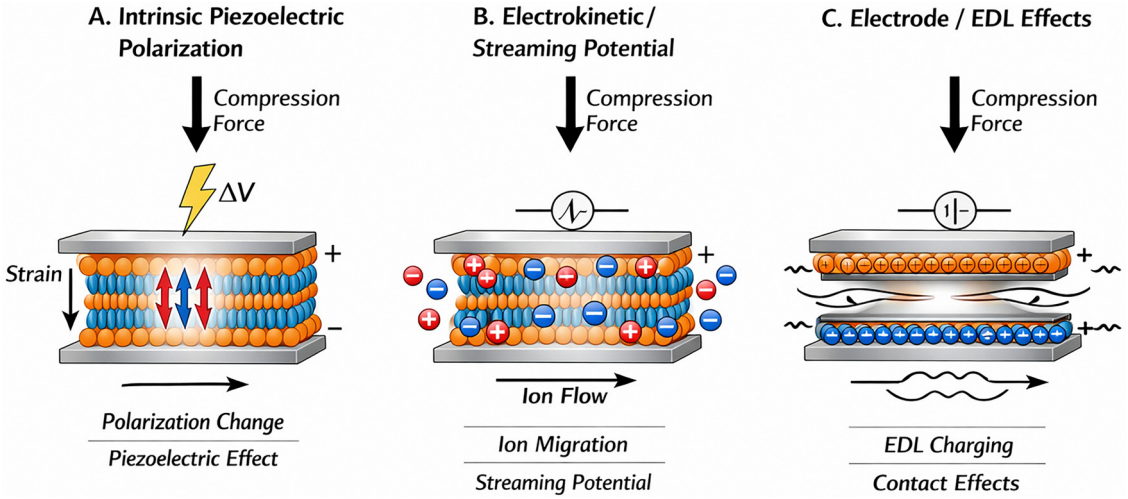

Fig. 2 Schematic representation of distinct physical mechanisms that can give rise to electrical signals under mechanical deformation in water-rich, ionically conductive amphiphile gels. (a) Intrinsic piezoelectric polarization, in which mechanical stress induces instantaneous reorientation of polar molecular units, leading to a strain-proportional electrical response. (b) Electrokinetic charge redistribution, where deformation drives relative motion of mobile ions and the gel matrix, producing transient voltage signals that relax as ionic equilibrium is restored. (c) Interfacial and electrode-related effects, including electrical double-layer charging and contact-area modulation at the gel–electrode interface, which can generate capacitive or transient electrical responses during mechanical loading. Although these mechanisms originate from fundamentally different microscopic processes, they can produce qualitatively similar experimental signatures—such as hysteretic cyclic voltammetry responses and mechanically induced voltage transients—highlighting the non-uniqueness of piezoelectric interpretations in hydrated, ionically conductive soft matter.

where P_p is the polarization density and d is an effective piezoelectric coefficient (units C N^{-1}).

Under open-circuit (high-input-impedance) readout—*i.e.*, negligible external current so that the measured signal corresponds to the internal field required to balance piezoelectrically generated bound charge—for a sample of thickness h and relative permittivity ε_r, the corresponding thickness voltage is (up to sign, which depends on electrode polarity and sign conventions):

$$V_p(t) = \frac{dh}{\varepsilon_0 \varepsilon_r} \sigma(t) \tag{3}$$

where ε_0 is the vacuum permittivity ($\approx 8.854 \times 10^{-12}$ F m^{-1}).

In this minimal description, V_p responds instantaneously to changes in $\sigma(t)$ and is weakly frequency-dependent within the elastic regime. If a constant stress state is maintained, V_p remains time-independent, reflecting the absence of intrinsic relaxation in purely elastic piezoelectric polarization.

4.3 Ionic and electrokinetic contribution

In hydrated, ionically conductive gels, mechanical deformation can drive redistribution of mobile ions relative to the (partly fixed-charge) network and the pore fluid, producing electrokinetic charge separation, space-charge buildup, and transient electrical signals. To capture this mechanism at a minimal, device-level (two-terminal) scale, we introduce an internal state variable $q_m(t)$, defined as the net mechanically induced electrode charge (units C) associated with ionic redistribution during deformation (*e.g.*, strain/pressure-driven ion transport and delayed space-charge relaxation).

We model the evolution of $q_m(t)$ phenomenologically as

$$\dot{q}_m(t) = \alpha \dot{\varepsilon}(t) - \frac{q_m(t)}{\tau} \tag{4}$$

where $\varepsilon(t)$ is the mechanical strain, $\dot{\varepsilon}(t)$ is the strain rate, α is a mechano-ionic coupling coefficient that converts a strain-rate input into electrode charge (units C, since $\alpha\,\dot{\varepsilon}$ must have units C s^{-1}), and τ is a characteristic ionic relaxation time (units s) set by ion mobility, solvent viscosity, and relevant structural length scales (*e.g.*, pore/mesh size and electrode separation). Eqn (4) encodes two key features: (i) mechanically driven charge generation scales primarily with strain rate, and (ii) the induced charge relaxes toward zero once deformation ceases.

The corresponding mechanically induced ionic/interfacial voltage contribution ($V_{m,I}$) to the measured electrode-to-electrode voltage is written as

$$V_{m,I}(t) = \frac{q_m(t)}{C_{eff}} \tag{5}$$

where C_{eff} is an effective capacitance (units F) that lumpingly incorporates the geometric capacitance of the sample and interfacial/double-layer (and contact) capacitances at the gel–electrode interfaces. This ionic/interfacial branch is therefore intrinsically rate-dependent and relaxational: it is driven primarily by $\dot{\varepsilon}(t)$ and, after a deformation event (*e.g.*, following unloading or during a controlled hold), relaxes as $q_m(t) \to 0$ on the timescale τ, consistent with experimentally observed post-event transients in hydrated ionic gels.

For gels containing redox-active species (including certain ionotropically crosslinked gels), an additional faradaic contribution may coexist with capacitive charging. In a minimal extension, this can be represented by adding a parallel

charge-transfer element in parallel with C_{eff}, whose faradaic current depends on the interfacial voltage drop $\Delta V_{\mathrm{int}}(t)$, *i.e.*, $I_{\mathrm{F}}(\Delta V_{\mathrm{int}}(t))$. In a lumped two-terminal description, $\Delta V_{\mathrm{int}}(t)$ is taken to be proportional to the measured open-circuit electrode-to-electrode voltage $V_{\mathrm{oc}}(t)$,

$$\Delta V_{\mathrm{int}}(t) = \beta V_{\mathrm{oc}}(t), \quad 0 < \beta < 1 \tag{6}$$

reflecting that only a fraction of the total voltage drop appears across the charge-transfer interface (with the remainder distributed across the bulk and/or the opposing electrode interface). Importantly, this extension introduces interfacial redox/leakage currents without altering the central separation between an instantaneous elastic polarization contribution and a relaxational ionic/interfacial contribution: $V_{\mathrm{m,I}}(t) = q_{\mathrm{m}}(t)/C_{\mathrm{eff}}$ denotes the mechanically induced ionic/interfacial component of the two-terminal voltage, whereas $\Delta V_{\mathrm{int}}(t)$ denotes the local interfacial voltage drop that governs charge-transfer kinetics.

4.4 Total electromechanical response

Under open-circuit (high-input-impedance, *i.e.*, instrument input impedance ≫ sample impedance) readout, the measured voltage V_{oc} is taken as the superposition of intrinsic polarization V_{p} and mechanically driven ionic/interfacial contributions $V_{\mathrm{m,I}}$:

$$V_{\mathrm{oc}}(t) = V_{\mathrm{p}}(t) + V_{\mathrm{m,I}}(t) \tag{7}$$

This additive decomposition enables mechanisms to be distinguished through their characteristic temporal and frequency dependence.

4.5 Predicted signatures under common experimental protocols

4.5.1 Rapid strain step/ramp. For a rapid applied strain step, the imposed macroscopic strain is idealized as

$$\varepsilon(t) = \varepsilon_{\max} H(t) \tag{8}$$

where $\varepsilon(t)$ is the time-dependent imposed strain, $\varepsilon_{\max}$ is the strain amplitude (final strain level reached by the step), and $H(t)$ is the Heaviside step function ($H(t) = 0$ for $t < 0$, $H(t) = 1$ for $t \geq 0$). This representation corresponds to the limit of a rapid strain ramp whose rise time is short compared with the ionic relaxation time τ; in practice, strain is applied with a finite rise time, and eqn (8) represents the fast-ramp limit.

Under this idealization, the intrinsic term produces an immediate stress-tracking voltage change that persists so long as the stress state is maintained. In contrast, the mechanically driven ionic/interfacial contribution relaxes exponentially under held deformation (Fig. 3a):

$$V_{\mathrm{m,I}}(t) = V_{\mathrm{m,I,0}} e^{-t/\tau} \tag{9}$$

where $V_{\mathrm{m,I,0}}$ is the ionic/interfacial voltage immediately after the rapid deformation event. Here, τ is the characteristic ionic relaxation time (s) governing the return of the mechanically induced electrode charge $q_{\mathrm{m}}(t)$ (and thus $V_{\mathrm{m,I}}(t) = q_{\mathrm{m}}(t)/C_{\mathrm{eff}}$) toward equilibrium after deformation. Physically, τ reflects the timescale for mobile ions to redistribute through the gel and

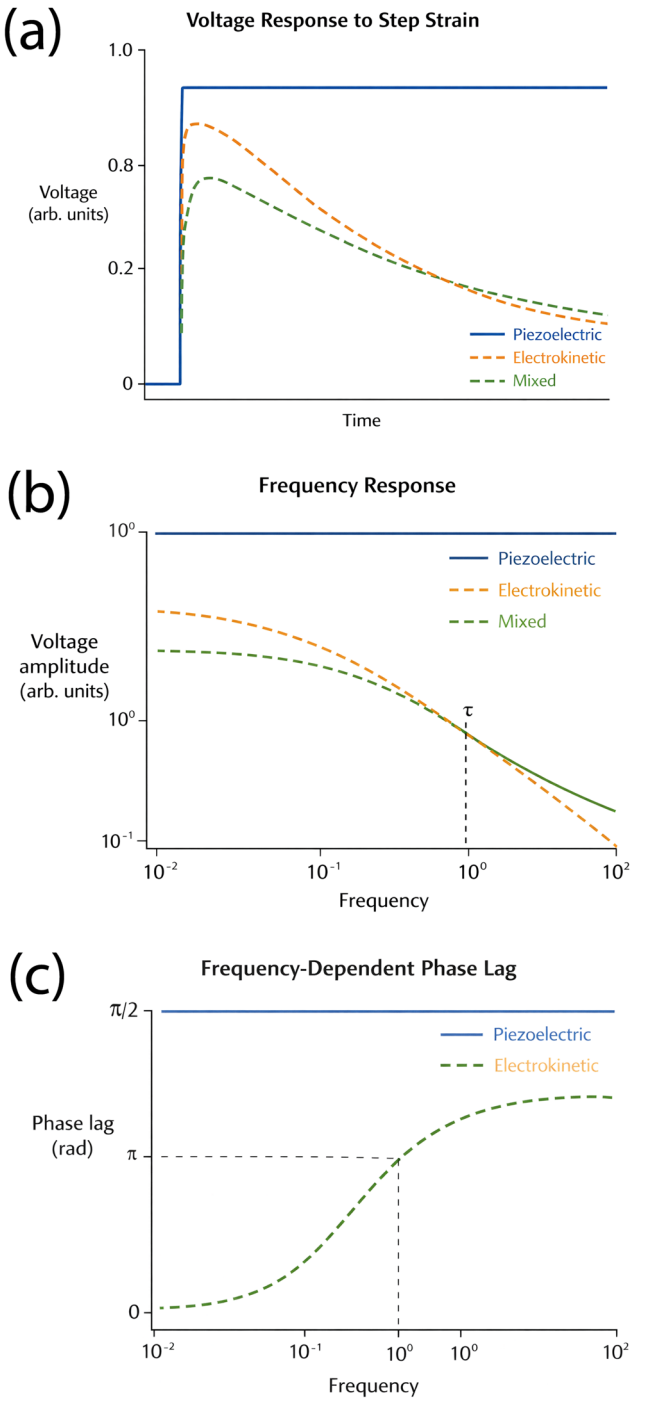

Fig. 3 Model-predicted electrical responses of hydrated ionic gels under representative mechanical loading protocols based on the coupled electromechanical framework described in Section 4. (a) Voltage response to a rapid strain step/ramp, showing the distinct signatures of intrinsic piezoelectric polarization (instantaneous response with no relaxation), electrokinetic contribution (transient response with exponential decay), and a mixed regime where both mechanisms coexist. (b) Frequency dependence of the voltage amplitude under sinusoidal strain, illustrating the frequency-independent response expected for intrinsic polarization and the dispersive roll-off associated with ionic relaxation characterized by a time constant τ. (c) Phase lag between applied strain and electrical response as a function of frequency, highlighting the negligible phase lag for intrinsic polarization and the increasing lag associated with electrokinetic contributions. Curves are generated from numerical integration of the minimal coupled electromechanical model using dimensionless parameters chosen to illustrate scaling behavior rather than to fit experimental data (see SI).

for interfacial polarization to relax, and it is set by ion mobility (or diffusivity), solvent viscosity, and relevant geometric/structural length scales (*e.g.*, pore/mesh size and electrode spacing).

For an ideal step, the relaxation term in eqn (4) is negligible during the impulse-like strain-rate event, so integrating eqn (4) across the step gives $\Delta q_m = \alpha\Delta\varepsilon = \alpha\varepsilon_{max}$, and therefore

$$V_{m,I,0} = \frac{\Delta q_m}{C_{eff}} = \frac{\alpha\varepsilon_{max}}{C_{eff}} \tag{10}$$

A transient signal followed by relaxation during a hold at fixed strain is therefore consistent with a dominant ionic/interfacial contribution, whereas a sustained stress-tracking plateau under controlled holding conditions suggests a substantial intrinsic polarization contribution.

4.5.2 Sinusoidal strain. For sinusoidal loading $\varepsilon(t) = \varepsilon_{max}\sin(\omega t)$, the intrinsic polarization response remains approximately frequency-independent within the elastic regime. Here, ω is the angular frequency ($\omega = 2\pi f$) and f is the loading frequency (Hz). The mechanically driven ionic/interfacial contribution exhibits strong frequency dispersion. Solving eqn (4) under steady-state sinusoidal loading yields the voltage amplitude

$$\left|V_{m,I}(\omega)\right| = \frac{\alpha\varepsilon_{max}\tau}{C_{eff}}\frac{\omega}{\sqrt{1+(\omega\tau)^2}} \tag{11}$$

and a phase shift relative to the applied strain of $\phi(\omega) = 90^\circ - \arctan(\omega\tau)$, *i.e.*, the ionic/interfacial contribution is approximately 90° out of phase with strain for $\omega\tau \ll 1$ and becomes approximately in phase with strain for $\omega\tau \gg 1$.

4.5.3 Cyclic voltammetry. To describe scan-rate-dependent hysteresis in cyclic voltammetry, we introduce a distinct slow ionic/interfacial polarization charge variable $q_e(t)$ (units C) driven by the applied potential sweep, separate from the mechanically driven charge state $q_m(t)$ in eqn (4). A minimal two-terminal representation is

$$I(t) = C_{eff}\dot{V}_{app}(t) + \dot{q}_e(t) \tag{12}$$

where $I(t)$ is the measured current, $V_{app}(t)$ is the applied electrode-to-electrode potential, and $\dot{V}_{app}(t)$ is the scan rate. The term $C_{eff}\dot{V}_{app}(t)$ captures effective capacitive charging (including geometric capacitance and interfacial/double-layer capacitance under the same electrode contact conditions), while $\dot{q}_e(t)$ represents the additional current associated with slow ionic/space-charge polarization and redistribution during the sweep. The kinetics of $q_e(t)$ are governed by ionic mobility and interfacial transport, and can be characterized by relaxation timescales comparable to τ (but not necessarily identical). Apparent offset currents near zero applied potential, scan-rate-dependent hysteresis, and strong electrode sensitivity can therefore occur without invoking ferroelectric switching, consistent with observations in hydrated amphiphile gels.

4.6 Limiting cases and physical interpretation

The framework admits clear limiting behaviors. In the limit $\alpha \to 0$, strain-rate–driven ionic charge separation vanishes and the electromechanical response reduces to the intrinsic polarization branch (*e.g.*, under open-circuit readout $V_{oc} \approx V_p$). Conversely, when $d \to 0$, the intrinsic polarization term vanishes ($V_p = 0$) and the measured signal is governed entirely by the ionic/interfacial branch, $V_{oc}(t) = V_{m,I}(t) = q_m(t)/C_{eff}$, *i.e.*, by strain-rate–driven ionic redistribution and interfacial/double-layer charging that relax with characteristic time τ. In realistic hydrated gels, both contributions may coexist, with their relative importance determined by composition, hydration level, ionic strength, electrode/interface state, and measurement protocol.

By explicitly separating instantaneous elastic polarization from rate-dependent ionic and interfacial effects, this minimal model provides a consistent interpretation of previously reported electromechanical signatures and establishes a quantitative basis for mechanism-discriminating experiments. The qualitative signatures predicted by the coupled framework under representative mechanical loading protocols are illustrated in Fig. 3. In particular, the model highlights how rapid strain step/hold experiments, frequency-dependent mechanical loading, and phase-sensitive measurements can distinguish between instantaneous polarization, relaxational ionic contributions, and mixed regimes. These trends follow directly from the scaling behavior of the governing equations and motivate the experimental strategies outlined in the following section.

4.7 Connection to standard piezoelectric observables and "apparent" coefficients

To facilitate comparison with conventional piezoelectric characterization, it is useful to relate the model parameters (d, α, τ, C_{eff})—where α and τ enter through the mechanically induced charge state $q_m(t)$ (eqn (4))—to experimentally reported charge- and voltage-based figures of merit.

An important figure is the charge-based coefficient determined under short-circuit and quasi-static charge sensing. In one-dimensional compression, the intrinsic polarization density is $P_p = d\sigma$ (eqn (2)). The corresponding polarization charge collected on electrodes of area A is

$$Q_p(t) = AP_p(t) = Ad\sigma(t) = dF(t) \tag{13}$$

where F is the total normal force (load). Using the nominal (area-averaged) stress definition $\sigma = F/A$ gives $F = \sigma A$. This recovers the standard charge coefficient definition under compression,

$$d_{33} \equiv \frac{Q_{meas}}{F} \tag{14}$$

where Q_{meas} denotes the measured electrode charge under the chosen charge-sensing protocol; for intrinsic polarization alone, $Q_{meas} = Q_p$.

Although uniaxial compression along the electrode normal is the standard configuration used to define and measure d_{33} *via* Q/F, in hydrated ionic gels mechanically driven ionic redistribution can contribute an additional, history-dependent electrode charge $q_m(t)$ (eqn (4)). Under charge-sensing conditions (*e.g.*, an electrometer or charge amplifier), the measured charge can therefore be written as

$$Q_{meas}(t) = Q_p(t) + q_m(t) \tag{15}$$

so that an apparent charge coefficient becomes protocol- and frequency-dependent:

$$d_{33}^{\mathrm{app}} \equiv \frac{Q_{\mathrm{meas}}}{F} = d + \frac{q_{\mathrm{m}}}{F} \tag{16}$$

Thus, in hydrated ionically conductive gels, Q/F should be interpreted as an apparent d_{33}^{app} unless ionic and interfacial contributions are independently ruled out.

Another important figure is the voltage-based coefficient estimated under open-circuit, high-input-impedance readout. For open-circuit measurements, the intrinsic voltage contribution is given by eqn (3) discussed earlier which corresponds to the standard voltage coefficient g_{33} defined by $E_3 = g_{33}\sigma$, with $E_3 = V/h$:

$$g_{33} = \frac{(V_{\mathrm{p}}/h)}{\sigma} = \frac{d}{\varepsilon_0 \varepsilon_{\mathrm{r}}} \tag{17}$$

In the coupled framework, the mechanically driven ionic/interfacial contribution adds

$$V_{\mathrm{m,I}}(t) = \frac{q_{\mathrm{m}}(t)}{C_{\mathrm{eff}}} \tag{18}$$

Therefore, the measured open-circuit voltage (eqn (6)) can be written as

$$V_{\mathrm{oc}}(t) = \underbrace{\frac{\mathrm{d}h}{\varepsilon_0 \varepsilon_{\mathrm{r}}}\sigma(t)}_{\text{intrinsic}} + \underbrace{\frac{q_{\mathrm{m}}(t)}{C_{\mathrm{eff}}}}_{\text{ionic/interfacial}} \tag{19}$$

Because C_{eff} includes geometric and interfacial/double-layer capacitances, changes in electrode material, wetting, or interfacial state can modify $V_{\mathrm{m,I}}$ (and thus any inferred "g_{33}") even if d is unchanged.

In summary, apparent piezoelectricity is protocol dependent. Under slow or quasi-static mechanical protocols, the ionic branch relaxes ($q_{\mathrm{m}} \to 0$ on the timescale τ), so charge- and voltage-based coefficients approach intrinsic limits set by d (if $d \neq 0$). Under faster loading or at frequencies $\omega\tau \gtrsim 1$, $q_{\mathrm{m}}(t)$ can remain out of equilibrium and contribute significantly, yielding dispersive, phase-shifted apparent coefficients $d_{33}^{\mathrm{app}}(\omega)$ and $g_{33}^{\mathrm{app}}(\omega)$ governed by α, τ, and C_{eff}. This mapping motivates the mechanism-discriminating experiments in Section 5, where the goal is to determine whether measured Q_{meas} and V_{oc} primarily track the intrinsic parameter d or the relaxational ionic/interfacial parameters α, τ, and C_{eff} (and their dependence on ionic environment and interfacial conditions).

5. Mechanism-discriminating experimental strategies

The minimal coupled electromechanical framework introduced above provides a clear basis for distinguishing intrinsic piezoelectric polarization from ionic and interfacial contributions in hydrated amphiphile gels and ionically conductive, crosslinked polymer (polyelectrolyte) gels. Importantly, the two mechanisms predict qualitatively different dependencies on frequency, loading protocol, ionic environment, and electrode properties. The experiments outlined below are therefore designed not to further characterize the materials *per se*, but to resolve the dominant physical origin of electromechanical transduction by selectively probing the parameters d, α, τ, and C_{eff} in the model.

5.1 Frequency- and rate-dependent mechanical loading

Dynamic mechanical loading experiments under controlled strain amplitude and frequency provide a direct means of separating instantaneous polarization from relaxational ionic effects. Measurements should be performed under both open-circuit (voltage) and short-circuit (current) conditions while subjecting the gel to sinusoidal or stepwise compressive deformation over a broad frequency range.

Within the model, intrinsic piezoelectric polarization contributes a response proportional to stress (or strain in the linear regime) and is therefore expected to exhibit weak frequency dependence within the elastic regime. In contrast, the ionic contribution scales with strain rate and is governed by the relaxation time τ, leading to strong attenuation and phase lag at frequencies $\omega \gg 1/\tau$. Observation of pronounced frequency dispersion and/or phase shifts in the electrical signal therefore implicates a dominant electrokinetic/interfacial contribution.

Step- or ramp-strain experiments provide an especially clear discriminator. Under a rapid deformation event followed by a controlled hold (or, more generally, by a defined post-event observation window), intrinsic polarization produces a sustained stress-tracking voltage/charge contribution, whereas ionic contributions relax with characteristic time τ. The presence or absence of relaxational evolution in the electrical signal after a deformation event directly maps onto the relative importance of the two mechanisms. As illustrated by the model predictions in Fig. 3b and c, frequency-dependent amplitude attenuation and phase lag provide particularly sensitive indicators for distinguishing intrinsic polarization from electrokinetic contributions in hydrated ionic gels.

5.2 Electrochemical impedance spectroscopy (EIS)

Electrochemical impedance spectroscopy (EIS) provides a frequency-resolved electrical fingerprint of hydrated ionic gels and is particularly useful here because it can independently quantify the interfacial and bulk elements that condition the "ionic branch" of the coupled framework (Section 4). In practice, EIS can (i) separate bulk ionic conduction from electrode polarization/double-layer charging, (ii) constrain the effective capacitance C_{eff} (including interfacial contributions), and (iii) identify characteristic relaxation frequencies associated with interfacial polarization and distributed ionic transport. These quantities are central to interpreting cyclic voltammetry hysteresis and mechanically induced transients, since both can be dominated by interfacial charging and delayed ionic redistribution even in the absence of intrinsic polarization.

A practical implementation for hydrated gels is to sandwich the specimen between electrodes of well-defined area and compliance, apply a small-amplitude sinusoidal perturbation (to remain in the linear regime), and record the complex

impedance over a broad frequency window (mHz–kHz or higher where feasible). Because soft ionic gels are susceptible to contact artifacts, EIS should be repeated under systematically varied electrode/interface conditions, including (i) different electrode materials and surface roughness, (ii) controlled contact pressure or pre-compression, and (iii) blocking *versus* non-blocking interfaces (*e.g.*, thin dielectric coatings) where feasible. Strong sensitivity of the impedance spectrum to electrode chemistry, wetting, or contact conformity indicates that the low-frequency response is dominated by interfacial polarization and contact impedance rather than bulk intrinsic polarization.

For analysis, the goal is mechanism discrimination rather than exhaustive equivalent-circuit fitting. Minimal, physically interpretable representations are preferred, typically including a bulk resistive pathway (effective ionic resistance) in series with an interfacial capacitive element (often dispersive and therefore captured by a constant-phase element), with optional distributed polarization/transport terms when needed. In hydrated ionic materials, the emergence of pronounced low-frequency dispersion and large apparent capacitance is commonly consistent with electrode polarization and/or space-charge (Maxwell–Wagner–Sillars-type) interfacial polarization. Mapping how these features shift with ionic strength, electrolyte composition, hydration, temperature, and static compression provides a direct route to constraining C_{eff} and identifying whether changes in mechanoelectric readouts are more plausibly attributed to altered ionic mobility/transport and interfacial charging rather than changes in an intrinsic coefficient d.

Finally, EIS pairs naturally with the mechanical protocols described in Sections 5.1 and 5.6. Recording spectra at different static strains (or before/after cyclic loading) can determine whether deformation primarily changes bulk conduction pathways (*via* porosity/permeability and ion mobility) or instead modulates the electrode interface (*via* wetting, conformity, and double-layer capacitance). This linkage provides an important cross-check when mechanically induced voltage/current transients could arise from contact-area modulation or deformation-driven ion redistribution.

5.3 Time-domain electrochemical step tests (chronoamperometry and chronopotentiometry)

Time-domain electrochemical step tests provide a direct complement to CV and EIS by converting interfacial charging and ionic polarization into explicit transient responses with identifiable time constants. In chronoamperometry, a small applied potential step is imposed across the gel–electrode stack and the current transient $I(t)$ is recorded. An instrument-limited prompt component reflects effective capacitive charging (constraining C_{eff} under the same contact conditions used in mechanoelectric tests), while slower decays quantify ionic/space-charge relaxation processes; any nonzero long-time current indicates leakage and/or faradaic contributions. In chronopotentiometry, a small current step is applied and the resulting voltage $V(t)$ is monitored; strong electrode dependence, drift, and nonlinearities (including polarity asymmetry) diagnose electrode polarization and interfacial impedance.

Mechanistically, these step-response measurements test whether the electrical dynamics are dominated by ionic/interfacial processes (large electrode and ionic-strength sensitivity; slow relaxation tails) *versus* requiring an intrinsic polarization term. Repeating chronoamperometry/chronopotentiometry across electrode materials, under blocking *versus* non-blocking interfaces, and as a function of ionic strength provides a stringent evaluation of whether time-domain electrical behavior is governed primarily by interfacial charging and ionic redistribution rather than intrinsic polarization.

5.4 Electrode blocking and interfacial control

Because electrokinetic and capacitive effects depend strongly on charge exchange and polarization at the electrode interface, electromechanical measurements should be repeated using both blocking and non-blocking electrodes. Blocking electrodes may be realized through thin dielectric coatings that suppress ion transfer while allowing displacement currents.

In the framework of Section 4, suppression of ionic exchange at the electrode interface should significantly reduce the mechanically driven ionic/interfacial contribution associated with $q_{\mathrm{m}}(t)$ and C_{eff}, while leaving any intrinsic piezoelectric response largely unaffected. Conversely, strong attenuation of the electromechanical signal under blocking conditions would implicate interfacial or electrokinetic origins.

Additional insight may be gained by systematically varying electrode material, surface roughness, and contact area. True intrinsic polarization contributions should scale predictably with sample geometry and applied stress, whereas interfacial effects often exhibit strong sensitivity to electrode chemistry and contact conditions.

5.5 Ionic strength and compositional dependence

Electromechanical measurements as a function of ionic strength and electrolyte composition provide a direct route to constraining the electrokinetic coupling parameter α and the ionic relaxation time τ in the coupled framework. Ionic strength can be tuned by adding nominally inert salts or by varying the counterion content intrinsic to the gel formulation; these perturbations primarily alter conductivity, screening length, and ion mobility, and therefore the rate and extent of strain-driven charge redistribution, while only secondarily affecting elasticity over moderate concentration ranges.

A caveat is that in self-assembled amphiphile gels, salts can also modify mesoscale order and mechanics (*e.g.*, domain spacing, anisotropy, porosity/permeability, and viscoelastic relaxation).[9,49,50] To preserve interpretability, ionic-strength sweeps should therefore be paired with concurrent structural/mechanical readouts (*e.g.*, small- and wide-angle X-ray scattering, SAXS/WAXS, or polarized light microscopy to probe mesophase order, and rheology to probe viscoelasticity) so that changes in electrical response can be mapped onto α, τ, and C_{eff} at approximately fixed structure, or else explicitly interpreted as coupled structure–transport effects. Where feasible,

"structure-preserving" electrolytes and modest concentration ranges should be used, and mechanical properties (*e.g.*, E and η) should be reported alongside at least one structural metric. This pairing helps separate primarily transport-driven ionic-strength effects from salt-induced structural changes.

Within the framework of Section 4, an intrinsic polarization contribution (parameterized by d) is expected to be comparatively insensitive to modest changes in ionic strength provided that mesoscale organization and elastic response are not substantially altered by the added electrolyte. In contrast, electrokinetic and interfacial pathways depend strongly on ion concentration, speciation, and transport. Consequently, substantial changes in signal magnitude, relaxational evolution after deformation events, phase lag, or frequency dispersion with ionic strength—especially when accompanied by minimal changes in rheology/structure—implicate dominant ionic/interfacial contributions (changes in α, τ, and C_{eff}). Comparisons across chemically distinct gels with similar mechanics but different ionic character offer an additional lever for separating mesoscale structure from ionic transport propensity, differentiating between intrinsic and electrokinetic mechanisms.

To emphasize that the electrical signatures discussed above are not specific to amphiphile mesophases, an instructive comparator is ionotropically crosslinked polyelectrolyte hydrogels. Carboxymethyl cellulose (CMC), a carboxylate-bearing polysaccharide, forms cohesive networks upon coordination with Cu^{2+}.[10] Under applied pressure, CMC gels crosslinked using $CuCl_2$ generate reproducible electrical signals with a stable response under repeated loading and exhibit hysteretic current–voltage loops under cyclic voltammetry, including measurable current near zero applied potential—features not observed for CMC in the absence of Cu salts.[10] A key additional observation is strong dependence on the counter-anion: gels prepared at comparable Cu^{2+} concentrations using $CuSO_4$ display substantially weaker electromechanical and CV signatures than those prepared with $CuCl_2$.[10] This anion sensitivity is consistent with an electrokinetic/interfacial interpretation: anion-dependent Cu^{2+} speciation and coordination, gel microstructure, and double-layer structure at the electrode interface can shift τ, α, and C_{eff}, thereby changing both mechanical-transient and CV responses without requiring changes in intrinsic polarization. The CMC–Cu^{2+} case therefore complements the amphiphile systems by demonstrating that the same phenomenology can arise in a chemically distinct, non-amphiphile hydrated ionic gel when multivalent ions and their counterions are present.

5.6 Hydration, temperature, and solvent mobility

Because ionic transport in hydrated gels depends on solvent viscosity and mobility, electromechanical responses should be examined as a function of hydration level and temperature. Within the coupled framework (Section 4), such changes primarily affect the ionic relaxation time τ (through ion mobility and solvent viscosity) and can also shift the effective capacitance C_{eff} *via* temperature-dependent double-layer structure and electrode polarization, whereas an intrinsic polarization contribution depends predominantly on elastic deformation.

Experimentally, temperature can strongly modulate measured signals in amphiphile gels. For example, in surfactant–fatty alcohol hydrogels, Patel *et al.* observed systematic temperature dependence of mechanically induced voltage transients, with the response decreasing upon heating and recovering after cooling, alongside qualitative weakening of the gel at elevated temperature.[12] This illustrates that temperature ramps can simultaneously perturb (i) ionic transport and interfacial charging and (ii) the gel's mesoscale organization and mechanical integrity.

Importantly, temperature can modulate the measured mechanoelectric output through multiple coupled pathways. Beyond changing ion mobility and solvent viscosity (thereby shifting τ and C_{eff}), heating can also affect self-assembly[51–55] and induce phase transitions,[56,57] thereby altering mesoscale order and mechanical integrity.[58]

As a result, heating can reshape strain localization, electrode contact conditions, and electromechanical readouts. Consequently, temperature dependence need not be monotonic or universal across formulations and should be interpreted alongside concurrent structural/mechanical readouts (*e.g.*, scattering or polarized light microscopy to track mesophase order, and rheology to track viscoelastic parameters such as E and η). A strong correlation between electrical signal magnitude or relaxation behavior and solvent mobility would support an electrokinetic/interfacial interpretation. Partial substitution of water with higher-viscosity solvents may provide additional insight, provided that the underlying self-assembled structure is preserved. Finally, while some crystalline polar materials are also pyroelectric, temperature-dependent signals in ionically conductive gels should not be taken as evidence of pyroelectric polarization unless a temperature-driven polarization change is independently demonstrated under controlled electrical boundary conditions (*e.g.*, heating/cooling transients in the absence of mechanical loading and with careful control of interfacial/ionic artifacts).

5.7 Quasi-static polarization measurements (direct charge–stress methods)

Where experimentally feasible, direct charge–stress measurements provide a stringent test for intrinsic piezoelectricity because they target the direct electromechanical effect (stress-induced charge) under controlled electrical boundary conditions, rather than inferring polarization from loop shapes or transient voltages. In practice, these measurements are typically implemented in a short-circuit/charge-amplifier configuration (sometimes termed "direct" or "quasi-static" d measurement, including Berlincourt-type approaches[59]), in which the electrodes are held near virtual ground and stress-induced charge is collected and quantified.[60] This configuration reduces ambiguity associated with unknown effective capacitances and interfacial voltage division, which can complicate open-circuit readouts.[59]

Although the example below is based on open-circuit-potential measurements rather than direct charge collection, it illustrates the broader point that perturbation-based tests can

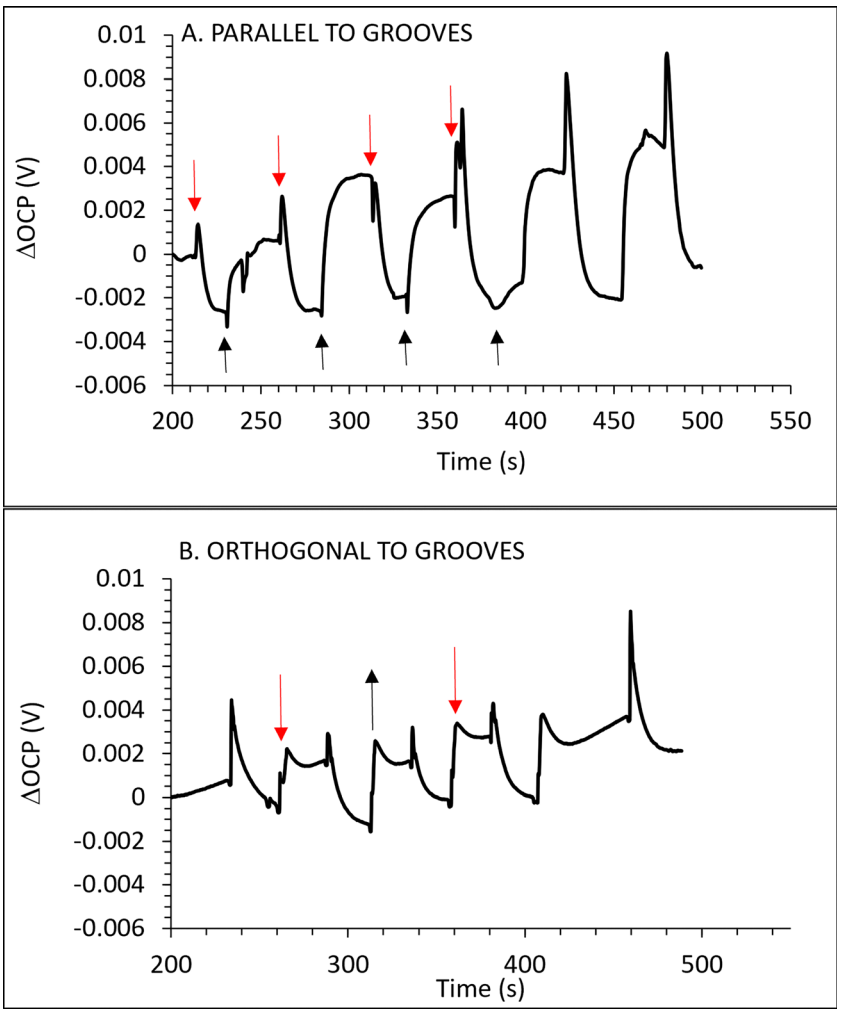

Fig. 4 Representative baseline-corrected OCP traces for an equimolar arginine–dodecanoic acid paste in water confined between grooved Al electrodes during repeated shear. Black and red arrows denote upward and downward shear strokes, respectively. (A) When shear is applied parallel to the grooves, opposite stroke directions produce distinguishable transient signatures. (B) When shear is applied orthogonally to the grooves, measurable transients remain, but directional resolution is lost. Representative traces were obtained for the same formulation under otherwise comparable measurement conditions.

help distinguish interfacial from putatively intrinsic electromechanical responses. As an illustrative example, we consider a hydrated arginine–dodecanoic acid paste confined between grooved aluminum electrodes, for which the interfacial boundary condition was deliberately varied while the material composition and measurement configuration were otherwise kept unchanged (Fig. 4). When shear was applied parallel to the grooves, opposite stroke directions produced distinguishable open-circuit-potential transients (Fig. 4A). In contrast, when shear was applied orthogonally to the grooves, a measurable mechanoelectric response remained, but directional resolution was lost (Fig. 4B). This behavior indicates that the measured response is strongly conditioned by anisotropic electrode/interface coupling, rather than reflecting a purely bulk electromechanical property that is independent of boundary alignment. We therefore view this type of boundary-condition perturbation as a practical way to test whether interfacial contributions are central to the observed mechanoelectric output. The full experimental study will be reported elsewhere; only a minimal representative subset is included here to illustrate the practical use of the present discrimination strategy.

A related conclusion emerges from published CMC hydrogel results, in which the electromechanical response depended strongly on the ionic crosslinking environment.[10] Taken together, these examples show that perturbation of either boundary conditions or ionic composition can materially alter the measured response, consistent with a substantial role for interfacial and electrokinetic contributions in hydrated ionic systems.

5.8 Connection to standard piezoelectric observables and "apparent" coefficients

A practical implementation for hydrated gels is as follows. The specimen is sandwiched between electrodes with well-defined area and compliance, mounted in a mechanical test frame (*e.g.*, an Instron-type universal testing machine) or a dynamic mechanical analyzer (DMA) equipped with a calibrated load

cell, and connected to a low-leakage charge amplifier/electrometer with guarding and shielding to suppress drift and triboelectric pickup. A controlled compressive force (or stress) is applied in small-amplitude cycles within the linear regime. The effective direct coefficient is obtained from the proportionality between collected charge and applied force over repeated cycles, with careful subtraction of baseline drift and verification of linearity.

For hydrated ionic gels, the key interpretive point is timescale (Section 4.7): intrinsic polarization contributes an effectively instantaneous, polarity-consistent charge increment that tracks applied loading, whereas electrokinetic/interfacial contributions are generally rate-dependent and relaxational, producing delayed charge accumulation, drift under held load, and/or post-event evolution associated with $q_m(t)$. Accordingly, the most diagnostic protocol is often not truly DC loading, but rather controlled step- or low-frequency loading combined with a time-windowed analysis: quantify the prompt charge increment upon loading/unloading, and separately assess any subsequent time-dependent evolution over a defined observation window. A robust intrinsic contribution should (i) scale linearly with force/stress over a range of small amplitudes, (ii) show consistent polarity under repeat cycling, and (iii) remain comparatively insensitive to modest changes in ionic strength and electrode blocking when gel structure and mechanics are held fixed. By contrast, strong dependence on loading rate, electrode condition, ionic strength, or pronounced relaxational evolution is more consistent with dominant ionic/interfacial mechanisms.[61,62]

Two additional practical cautions are particularly important in soft, conductive gels. First, finite gel conductivity can shunt charge on the measurement timescale, limiting the effective ''quasi-static'' window and making high insulation and guarding essential (otherwise the experiment becomes a measurement of leakage and interfacial polarization rather than direct piezoelectric charge). Second, because many soft contacts are compliance- and wetting-sensitive, the electrode stack should be designed to minimize changes in real contact area with load (or to monitor it), since contact evolution can generate apparent charge transients even without bulk polarization. Together with the mapping in Section 4.7, quasi-static (or low-frequency) charge collection with a well-defined time window---distinguishing the prompt response from any subsequent evolution—offers a practical way to separate an instantaneous polarization contribution from rate-dependent ionic redistribution and interfacial charging in these water-rich, conductive materials.

5.9 Mapping experiments onto the coupled framework

Crucially, the experiments described above are not independent probes, but complementary tests of the same minimal framework (Section 4) that jointly constrain the parameters governing instantaneous polarization, ionic redistribution, and interfacial charging. Frequency- and rate-dependent mechanical loading primarily constrains the ionic relaxation time τ through the onset of amplitude roll-off and phase lag, whereas ionic-strength and electrolyte-composition sweeps predominantly modulate the electrokinetic coupling α and the effective capacitance C_{eff} *via* changes in conductivity, screening, and double-layer structure. Quasi-static direct charge–stress measurements, when implemented under controlled electrical boundary conditions and sufficiently slow protocols, provide the most direct route to estimating an effective intrinsic coupling (*i.e.*, d-like behavior) because they minimize strain-rate-driven ionic currents and emphasize polarity-consistent charge generation under load reversal.

EIS provides an essential electrical ''bridge'' between the mechanically driven measurements and the voltage/current readouts by independently quantifying the interfacial and bulk electrical elements that set C_{eff} and relevant relaxation frequencies. In practice, EIS can be used to (i) determine whether the low-frequency response is dominated by electrode polarization/contact impedance, (ii) establish how C_{eff} and bulk resistance vary with hydration, temperature, ionic strength, and static compression, and (iii) identify whether timescales inferred from mechanoelectric relaxation are consistent with electrically measured relaxation processes (interfacial polarization *versus* bulk transport). Consistency across these orthogonal measurements strengthens a mechanistic assignment; inconsistency is itself diagnostic and often points to interface-dominated artifacts or protocol-dependent boundary conditions. Time-domain step tests (chronoamperometry/chronopotentiometry) complement this bridge by providing explicit transient relaxation signatures under controlled electrical perturbations, enabling cross-validation of τ-like timescales and the extent of electrode polarization.

A practical workflow is therefore to treat each formulation as a point in a low-dimensional parameter space (d,α,τ,C_{eff}) rather than as an *a priori* ''piezoelectric'' or ''non-piezoelectric'' class. Specifically: (i) use EIS (and time-domain step tests where relevant) to establish whether the electrical response is bulk- or interface-dominated and to parameterize C_{eff} (and bulk resistance) under the same contact conditions used for mechanoelectric tests; (ii) use step/ramp strain and sinusoidal loading to extract τ from relaxational evolution and phase/amplitude dispersion; (iii) use ionic-strength/composition sweeps to test whether changes in electrical output co-vary with conductivity and double-layer signatures (implicating α, τ, C_{eff}) or instead persist under nearly fixed electrical spectra (supporting a larger intrinsic component); and (iv) use quasi-static charge–stress protocols to test for polarity-consistent, rate-insensitive charge generation that scales with applied force and sample geometry. Where salts or temperature also modify mesoscale structure and mechanics, concurrent rheology/structural readouts should be used to distinguish transport-dominated changes in α, τ, C_{eff} from structure-mediated changes that can modulate both ionic pathways and any effective intrinsic coupling.

By integrating these measurements, it becomes possible to report mechanism-resolved figures of merit—*e.g.*, the fraction of the signal attributable to relaxational ionic dynamics under a specified protocol, the characteristic τ and its dependence on hydration/temperature, and the sensitivity of C_{eff} to electrode/

interface conditions—rather than relying on CV hysteresis or stress-generated transients alone. Such a mechanism-resolved approach is essential for interpreting electromechanical signals in hydrated ionic gels and for guiding the rational design of soft electromechanical materials, because it identifies which design levers (mesoscale order, ion content, hydration, electrode/interface engineering) control performance under the intended operating frequency and boundary conditions.

6. Implications for soft electromechanical materials

The reassessment presented here has implications that extend beyond the specific amphiphile gels considered. More broadly, it highlights the need for mechanism-resolved descriptions of electromechanical coupling in soft, hydrated, and ionically conductive materials. In such systems, electrical responses to mechanical deformation need not arise from a single constitutive mechanism, but may instead reflect the superposition of intrinsic polarization, electrokinetic charge redistribution, and interfacial effects. Accordingly, reporting electromechanical performance should be accompanied by protocols that identify which pathway dominates under the intended operating conditions.

From an applications perspective, this distinction is not merely semantic. Regardless of whether intrinsic piezoelectricity ultimately dominates in a given formulation, the ability of water-rich gels to reproducibly convert mechanical deformation into electrical signals positions them as promising candidates for soft sensors, biointerfaces, and mechanically responsive scaffolds. In many biomedical contexts, compliance, hydration, and ionic conductivity are advantageous features rather than limitations, and electromechanical transduction mediated by ionic processes may be equally, or even more, relevant than classical piezoelectricity.

The framework developed here also suggests that electromechanical responses in biological tissues—often described as piezoelectric—may similarly reflect coupled ionic and interfacial mechanisms in addition to any intrinsic polarization. In this light, hydrated amphiphile gels provide a useful model system for exploring how structural organization, ionic transport, and mechanics interact to produce electrical signals in soft matter. Rather than seeking to replicate rigid piezoelectric crystals in aqueous environments, it may be more fruitful to embrace the distinctive electromechanical pathways enabled by hydration and ionic mobility.

Finally, by explicitly separating intrinsic and extrinsic contributions, the present analysis provides design principles for tailoring electromechanical performance. Maximizing an intrinsic polarization contribution requires promoting stable polar/anisotropic organization while minimizing ionic/interfacial contributions on the measurement timescale (*e.g.*, through reduced conductivity, blocking interfaces, or appropriate operating frequencies). Conversely, exploiting electrokinetic pathways favors high mobile-ion content and transport, coupled with mesoscale anisotropy and deliberately engineered interfaces that control double-layer charging and contact impedance. These considerations open routes for engineering soft electromechanical materials with application-specific response characteristics and for comparing systems on a mechanism-resolved basis rather than by categorical labels alone.

7. Conclusions

We have presented a mechanistic reassessment of the electromechanical behavior reported for a class of water-rich, self-assembled amphiphile gels previously described as piezoelectric. By synthesizing observations across multiple chemically distinct systems, we show that capacitive cyclic voltammetry responses and mechanically induced electrical signals are robust and reproducible features of these materials. At the same time, we show that these signatures are not uniquely diagnostic of intrinsic piezoelectric polarization in hydrated, ionically conductive soft matter, because comparable readouts can arise from electrokinetic charge redistribution and gel–electrode interfacial charging.

To address this ambiguity, we introduced a minimal coupled electromechanical framework that explicitly separates instantaneous elastic polarization from rate-dependent ionic and interfacial contributions. This model rationalizes key experimental observations and predicts distinct temporal and frequency-dependent signatures that enable mechanism discrimination. Building on this framework, we outlined a set of targeted experimental strategies—combining frequency- and rate-dependent mechanical loading with impedance-based and time-domain electrochemical controls (EIS, chronoamperometry, and chronopotentiometry), electrode blocking, and ionic-strength perturbations—required to resolve the relative contributions of intrinsic and electrokinetic pathways in future studies. In particular, chronoamperometry and chronopotentiometry provide direct time-domain probes of interfacial charging and slow ionic polarization through current- and voltage-transient kinetics, offering independent constraints on relaxation timescales and leakage/faradaic contributions that can otherwise masquerade as piezoelectric-like signatures.

This reassessment does not diminish the functional relevance of amphiphile-based hydrogels as electromechanically responsive materials. Rather, it provides a rigorous, mechanism-resolved foundation for understanding and exploiting their behavior, whether the dominant pathway is intrinsic polarization, electrokinetic coupling, interfacial effects, or a superposition thereof. By clarifying how electrical signals emerge under mechanical deformation in water-rich gels, this work enables more defensible performance comparisons and supports the rational design of soft electromechanical transducers for sensing, biointerfacing, and biomedical applications.

Conflicts of interest

There are no conflicts to declare.

Data availability

The Python script used to generate the model predictions shown in Fig. 2 is supplied here: Pensini, Erica, 2026, ''Python code for simulations of piezoelectric model'', https://doi.org/10.7910/DVN/JNJLWG, Harvard Dataverse, V1. Data will also be made available upon reasonable request to the corresponding author.

Supplementary information (SI) is available. This Supporting Information presents the numerical methods underlying the coupled electromechanical model and provides code availability details for the simulations used to generate the representative responses shown in the manuscript. See DOI: https://doi.org/10.1039/d6sm00047a.

Acknowledgements

We acknowledge the financial assistance of the Natural Sciences and Engineering Research Council of Canada to AGM (RGPIN049832020) and EP (RGPIN5378712023).

References

1 Q. Deng, L. Liu and P. Sharma, Electrets in soft materials: nonlinearity, size effects, and giant electromechanical coupling, *Phys. Rev. E: Stat., Nonlinear, Soft Matter Phys.*, 2014, **90**(1), 012603.
2 N. Zolfaghari, P. Khandagale, M. J. Ford, K. Dayal and C. Majidi, Network topologies dictate electromechanical coupling in liquid metal–elastomer composites, *Soft Matter*, 2020, **16**(38), 8818–8825.
3 C. Majidi, Soft-matter engineering for soft robotics, *Adv. Mater. Technol.*, 2019, **4**(2), 1800477.
4 M. Grasinger and K. Dayal, Statistical mechanical analysis of the electromechanical coupling in an electrically-responsive polymer chain, *Soft Matter*, 2020, **16**(27), 6265–6284.
5 W. Lu, W. L. Ong, X. Pan, Z. Li, G. Tian and G. W. Ho, Design Strategies and Roles of Hydrogels for Sustainable Energy Conversion and Harvesting from Natural and Biological Environments, *Adv. Mater.*, 2025, **37**(50), e10270.
6 Z. Chen, H. Wang, Y. Cao, Y. Chen, O. Akkus, H. Liu and C. C. Cao, Bio-inspired anisotropic hydrogels and their applications in soft actuators and robots, *Matter*, 2023, **6**(11), 3803–3837.
7 E. Pensini, S. Gregori, A. G. Marangoni, S. M. Ghazani, Z. Su, A. Chen and N. Kashlan, Ethanolamine piezoelectric hydrogels structured by oleic acid lamellae, *J. Mol. Liq.*, 2024, **397**, 124185.
8 E. Pensini, P. Meszaros, N. Kashlan, A. G. Marangoni, S. Gregori, S. M. Ghazani, J. van der Zalm and A. Chen, Ferroelectric soft materials formed with alkanolamines and unsaturated fatty acids, *J. Mol. Liq.*, 2025, **419**, 126823.
9 E. Pensini, P. Meszaros, N. Kashlan, A. G. Marangoni, T. Laredo, S. Gregori, S. M. Ghazani, J. van der Zalm and A. Chen, Ferroelectric hydrogels from amino acids and oleic acid, *iScience*, 2024, **27**(9), 110601.
10 E. Pensini and S. Gregori, Pressure Sensing Piezoelectric Hydrogels for Flexible Wearable Devices, *Medical Measurements & Applications (MeMeA)*, IEEE, Chania, Greece, 2025, pp. 1–5.
11 G. Alici, G. M. Spinks, J. D. Madden, Y. Wu and G. G. Wallace, Response characterization of electroactive polymers as mechanical sensors, *IEEE/ASME Trans. Mech.*, 2008, **13**(2), 187–196.
12 E. Patel, A. Chen, S. M. Ghazani, A. G. Marangoni, S. Gregori and E. Pensini, Piezoelectric crystalline hydrogels of two surfactants with different polarity and long-chain alcohols, *J. Mol. Liq.*, 2025, **435**, 128108.
13 K. Chen and D. Ho, Piezoionics: mechanical-to-ionic transduction for sensing, biointerface, and energy harvesting, *Aggregate*, 2024, **5**(1), e425.
14 G. W. Hastings and F. A. Mahmud, Electrical effects in bone, *J. Biomed. Eng.*, 1988, **10**(6), 515–521.
15 J. Wu, Understanding the electric double-layer structure, capacitance, and charging dynamics, *Chem. Rev.*, 2022, **122**(12), 10821–10859.
16 Y. Dobashi, D. Yao, Y. Petel, T. N. Nguyen, M. S. Sarwar, Y. Thabet, C. L. Ng, E. Scabeni Glitz, G. T. M. Nguyen and C. Plesse, *et al.*, Piezoionic mechanoreceptors: force-induced current generation in hydrogels, *Science*, 2022, **376**(6592), 502–507.
17 A. Al-Amodi and R. J. Hill, Streaming potentials of hyaluronic acid hydrogel films, *Langmuir*, 2022, **38**(44), 13370–13381.
18 A. P. Franco and A. L. Ramalho Mercê, Complexes of carboxymethylcellulose in water. 1: Cu^{2+}, VO^{2+} and Mo^{6+}, *React. Funct. Polym.*, 2006, **66**(6), 667–681.
19 H. Yan, R. Qi, Z. Liu, H. Wang, C. Dong and L. Z. Zhang, Unlocking the potential of hydrogel-electrode electrical double layer for high-performance moisture-enabled electric generators, *Device*, 2025, **3**(2), 100568.
20 A. Fiumefreddo and M. Utz, Bulk streaming potential in poly(acrylic acid)/poly(acrylamide) hydrogels, *Macromolecules*, 2010, **43**(13), 5814–5819.
21 C. Kopecz-Muller, V. Bertin, E. Raphaël, J. D. McGraw and T. Salez, Mechanical response of a thick poroelastic gel in contactless colloidal-probe rheology, *Proc. R. Soc. A*, 2023, **479**(2271), 20220832.
22 H. Wang and L. Pilon, Physical interpretation of cyclic voltammetry for measuring electric double layer capacitances, *Electrochim. Acta*, 2012, **64**, 130–139.
23 A. J. Bard, L. R. Faulkner and H. S. White, *Electrochemical methods: fundamentals and applications*, John Wiley & Sons, 2022.
24 B. J. Venton and Q. Cao, Fundamentals of Fast-Scan Cyclic Voltammetry for Dopamine Detection, *Analyst*, 2020, **145**(4), 1158–1168.
25 C. Amatore, Y. Bouret, E. Maisonhaute, H. D. Abruña and J. I. Goldsmith, Electrochemistry within molecules using ultrafast cyclic voltammetry, *C. R. Chim*, 2023, **6**(1), 99–115.
26 C. M. Schott, P. M. Schneider, K. T. Song, H. Yu, R. Götz, F. Haimerl, E. Gubanova, J. Zhou, T. O. Schmidt and Q. Zhang, *et al.*, How to Assess and Predict Electrical Double

Layer Properties. Implications for Electrocatalysis, *Chem. Rev.*, 2024, **124**(22), 12391–12462.

27 R. Baretta, G. Davidson-Rozenfeld, V. Gutkin, M. Frasconi and I. Willner, Chemical and Photochemical-Driven Dissipative Fe^{3+}/Fe^{2+}-Ion Cross-Linked Carboxymethyl Cellulose Gels Operating Under Aerobic Conditions: Applications for Transient Controlled Release and Mechanical Actuation, *J. Am. Chem. Soc.*, 2024, **146**(14), 9957–9966.

28 B. Taji, S. Shirmohammadi, V. Groza and I. Batkin, Impact of Skin–Electrode Interface on Electrocardiogram Measurements Using Conductive Textile Electrodes, *IEEE Trans. Instrum. Meas.*, 2013, **63**(6), 1412–1422.

29 F. Bordi, C. Cametti and T. Gili, Reduction of the contribution of electrode polarization effects in the radiowave dielectric measurements of highly conductive biological cell suspensions, *Bioelectrochemistry*, 2001, **54**(1), 53–61.

30 A. Koklu, A. C. Sabuncu and A. Beskok, Rough Gold Electrodes for Decreasing Impedance at the Electrolyte/Electrode Interface, *Electrochim. Acta*, 2016, **205**, 215–225.

31 L. Yang, L. Gan, Z. Zhang, Z. Zhang, H. Yang, Y. Zhang and J. Wu, Insight into the Contact Impedance between the Electrode and the Skin Surface for Electrophysical Recordings, *ACS Omega*, 2022, **7**(16), 13906–13912.

32 H. Xue, D. Wang, M. Jin, H. Gao, X. Wang, L. Xia, D. A. Li, K. Sun, H. Wang and X. Dong, *et al.*, Hydrogel electrodes with conductive and substrate-adhesive layers for noninvasive long-term EEG acquisition, *Microsyst. Nanoeng.*, 2023, **9**(1), 79.

33 W. Chen, J. Lin, Z. Ye, X. Wang, J. Shen and B. Wang, Customized surface adhesive and wettability properties of conformal electronic devices, *Mater. Horiz.*, 2024, **11**(24), 6289–6325.

34 Y. Lu, C. Z. Zhao, H. Yuan, X. B. Cheng, J. Q. Huang and Q. Zhang, Critical current density in solid-state lithium metal batteries: mechanism, influences, and strategies, *Adv. Funct. Mater.*, 2021, **31**(18), 2009925.

35 G. Li, S. Wang and Y. Y. Duan, Towards conductive-gel-free electrodes: understanding the wet electrode, semi-dry electrode and dry electrode-skin interface impedance using electrochemical impedance spectroscopy fitting, *Sens. Actuators, B*, 2018, **277**, 250–260.

36 M. Samet, V. Levchenko, G. Boiteux, G. Seytre, A. Kallel and A. Serghei, Electrode polarization vs. Maxwell-Wagner-Sillars interfacial polarization in dielectric spectra of materials: characteristic frequencies and scaling laws, *J. Chem. Phys.*, 2015, **142**, 194703.

37 I. Ahmad, M. J. Akhtar, M. Younas, M. Siddique and M. M. Hasan, Small polaronic hole hopping mechanism and Maxwell–Wagner relaxation in $NdFeO_3$, *J. Appl. Phys.*, 2012, **112**, 074105.

38 F. Tayari, K. I. Nassar, M. Benamara, M. Essid, S. S. Teixeira and M. P. F. Graça, Sol–gel synthesized $(Bi_{0.5}Ba_{0.5}Ag)_{0.5}$-$(NiMn)_{0.5}O_3$ perovskite ceramic: an exploration of its structural characteristics, dielectric properties and electrical conductivity, *Ceram. Int.*, 2024, **50**(7), 11207–11215.

39 S. Meloni, T. Moehl, W. Tress, M. Franckevičius, M. Saliba, Y. H. Lee, P. Gao, M. K. Nazeeruddin, S. M. Zakeeruddin and U. Rothlisberger, *et al.*, Ionic polarization-induced current–voltage hysteresis in $CH_3NH_3PbX_3$ perovskite solar cells, *Nat. Commun.*, 2016, **7**(1), 10334.

40 Y. G. Ro, S. Na, J. Kim, Y. Chang, S. Lee, M. S. Kwak, S. Jung and H. Ko, Iontronics: Neuromorphic Sensing and Energy Harvesting, *ACS Nano*, 2025, **19**(27), 24425–24507.

41 J. E. Potaufeux, J. Odent, D. Notta-Cuvier, F. Lauro and J. M. Raquez, A comprehensive review of the structures and properties of ionic polymeric materials, *Polym. Chem.*, 2020, **11**(37), 5914–5936.

42 A. V. Delgado, F. González-Caballero, R. J. Hunter, L. K. Koopal and J. Lyklema, Measurement and interpretation of electrokinetic phenomena, *J. Colloid Interface Sci.*, 2007, **309**(2), 194–224.

43 R. B. Schoch, J. Han and P. Renaud, Transport phenomena in nanofluidics, *Rev. Mod. Phys.*, 2008, **80**(3), 839–883.

44 T. Tanaka and D. J. Fillmore, Kinetics of swelling of gels, *J. Chem. Phys.*, 1979, **70**(3), 1214–1218.

45 P. Kohn, K. Schröter and T. Thurn-Albrecht, Interfacial Polarization and Field-Induced Orientation in Nanostructured Soft-Ion Conductors, *Phys. Rev. Lett.*, 2009, **102**(21), 216101.

46 Y. Jiang, Z. Liu, C. Wang and X. Chen, Heterogeneous strain distribution of elastomer substrates to enhance the sensitivity of stretchable strain sensors, *Acc. Chem. Res.*, 2019, **52**(1), 82–90.

47 T. Y. Kim, W. Suh and U. Jeong, Approaches to deformable physical sensors: electronic versus iontronic, *Mater. Sci. Eng., R*, 2021, **146**, 100640.

48 X. Chen, X. Xia and C. F. Guo, Flexible Iontronic Sensing: Ionic Materials, Electrodes, and Encapsulation, *Adv. Funct. Mater.*, 2025, e12920.

49 Z. Luo, B. Åkerman, S. Zhang and B. Nordén, Structures of self-assembled amphiphilic peptide-heterodimers: effects of concentration, pH, temperature and ionic strength, *Soft Matter*, 2010, **6**(10), 2260–2270.

50 Y. Jiang, T. Geng, Q. Li, G. Li and H. Ju, Influences of temperature, pH and salinity on the surface property and self-assembly of 1 : 1 salt-free catanionic surfactant, *J. Mol. Liq.*, 2014, **199**, 1–6.

51 Y. Wang, X. Gao, Y. Xiao, Q. Zhao, J. Yang, Y. Yan and J. Huang, Temperature dependent coordinating self-assembly, *Soft Matter*, 2015, **11**(14), 2806–2811.

52 N. Carl, W. Müller, R. Schweins and K. Huber, Controlling Self-Assembly with Light and Temperature, *Langmuir*, 2019, **36**(1), 223–231.

53 Z. Ye, H. Zhang, H. Luo, S. Wang, Q. Zhou, X. Du, C. Tang, L. Chen, J. Liu and Y. K. Shi, *et al.*, Temperature and pH effects on biophysical and morphological properties of self-assembling peptide RADA16-I, *J. Pept. Sci.*, 2008, **14**(2), 152–162.

54 A.-L. Fameau, A. Arnould and A. Saint-Jalmes, Responsive self-assemblies based on fatty acids, *Curr. Opin. Colloid Interface Sci.*, 2014, **19**(5), 471–479.

55 G. E. Cunningham, J. J. O'Sullivan and M. J. Simmons, Exploring formulation, manufacture and characterisation techniques of lamellar gel networks in hair conditioners: a review, *Adv. Colloid Interface Sci.*, 2025, **339**, 103419.

56 F. Schreiber, Structure and growth of self-assembling monolayers, *Prog. Surf. Sci.*, 2000, **65**(5–8), 151–257.
57 A. Yaghmur, B. Sartori and M. Rappolt, Self-assembled nanostructures of fully hydrated monoelaidin–elaidic acid and monoelaidin–oleic acid systems, *Langmuir*, 2012, **28**(26), 10105–10119.
58 Y. S. Dagdas, A. Tombuloglu, A. B. Tekinay, A. Dana and M. O. Guler, Interfiber interactions alter the stiffness of gels formed by supramolecular self-assembled nanofibers, *Soft Matter*, 2011, **7**(7), 3524–3532.
59 M. Stewart, W. Battrick and M. G. Cain, Measurement Good Practice Guide No. 44, in *Measuring piezoelectric d_{33} coefficents using the direct method, ed. N. P.,* Laboratory, Teddington, Middlesex, United Kingdom, 2001.
60 R. S. Muddam, S. Wang, N. P. Maria Joseph Raj, Q. Wang, P. Wijesinghe, J. Payne, M. S. Dyer, C. Bowen and L. Krishnan Jagadamma, Self-Poled Halide Perovskite Ruddlesden–Popper Ferroelectric–Photovoltaic Semiconductor Thin Films and Their Energy Harvesting Properties, *Adv. Funct. Mater.*, 2025, **35**(34), 2425192.
61 Y. Fang, H. Ouyang, Y. Cheng, Y. Zhou, L. Shi, J. Sun, G. W. Ho and R. Wang, Ultrasensitive multi-degree-of-freedom piezoionic sensor via synergistic hydrogel–ion interactions, *Nat. Commun.*, 2026, **17**, 893.
62 V. Woehling, G. T. Nguyen, C. Plesse, Y. Petel, Y. Dobashi, J. D. Madden, C. A. Michal and F. Vidal, Study of the piezoionic effect and influence of electrolyte in conducting polymer based soft strain sensors, *Multifunct. Mater.*, 2019, **2**(4), 045002.

